

## Scientific Session-10 Miscellaneous

World J Nucl Med 2009;8:259-263

094

### Molecular Radiotherapy for Human Neuroblastoma Cells with Auger Electrons of In-111-labeled N-myc Antisense Oligonucleotides in Combination with Chemotherapy

Dr. Naoyuki Watanabe  
NIRS, Chiba, Japan

Abstract not available

095

### Molecular Imaging and Therapy of Cancer Using Radiolabeled Nanoparticles

Keon Wook Kang<sup>1,2</sup>, Young-Hwa Kim<sup>1,2</sup>, Hyewon Youn<sup>1,2</sup>, Jun Sung Kim<sup>3</sup>, Yun-Sang Lee<sup>1,2</sup>, June-Key Chung<sup>1,2</sup>, Myung Chul Lee<sup>1</sup>, and Dong Soo Lee<sup>1</sup>

<sup>1</sup>Department of Nuclear Medicine, Seoul National University College of Medicine, <sup>2</sup>Laboratory of Molecular Imaging and Therapy, Cancer Research Institute, Seoul National University, & <sup>3</sup>Biterials Co., Ltd, Seoul, KOREA

Molecular imaging is used for earlier detection, characterization of disease and an earlier assessment of treatment efficacy through imaging molecular/cellular events in living organisms. For the imaging sources, fluorescent materials, radioisotopes, and MRI enhancers can be used. Each modality has its own advantages and limitations with respect to sensitivity, resolution, tissue penetration of signal, and etc. Multimodal technique combined PET/MRI/optical imaging will overcome the limitations of each modality. Recent advances in nanobiotechnology have identified many candidates for medical applications. Nanoparticles are able to carry fluorescent dye, radioisotope, drugs, genes, and targeting biomarkers on their surface and inside. These multifunction nanoparticles can be used for diagnostic in vitro and in vivo and therapeutic purpose as well. We combined multimodal molecular imaging technique with nanotechnology to manage cancer. We examined the feasibility of PET/MRI/fluorescent tri-modal imaging for sentinel lymph node detection using radiolabeled silica nanoparticles and molecular targeted imaging using liposome nanoparticle conjugated with SLX for cancer in mouse model.

#### Multimodal molecular imaging

We developed 50 nm sized amino PEGylated magnetic silica nanoparticles containing near infrared fluorescent dye, NIR-797 isothiocyanate and iron oxide core (TMSN-N50). We conjugated a chelating agent, 2-(p-isothiocyanatobenzyl)-1,4,7-triazacyclononane-1,4,7-triacetic acid (SCN-NOTA) to amine on the surface of TMSN-N50 and labeled a positron emitter, <sup>68</sup>Ga on SCN-NOTA-TMSN-N50 by adding <sup>68</sup>Ga eluted from a <sup>68</sup>Ge/<sup>68</sup>Ga generator. <sup>68</sup>Ga-SCN-NOTA-TMSN-N50 nanoparticles was injected subcutaneously into foot-pad on the leg of mice. Whole-body images were obtained using an animal PET/CT scanner (eXplore Vista DR PET/CT, GE Healthcare, Milwaukee, WI), animal MRI (7 T BioSpec, Bruker, Germany) and an in vivo optical imaging system (Maestro, CRI, Boston, MA). We fused PET and MRI image using an in-house registering software FIRE. We could observe draining axillary and brachial lymph nodes from PET, MRI and optical images (Fig 1). We also observe fluorescence signals ex vivo after dissecting the lymph node in gross and under the microscope.

We suggest that PET/MRI/fluorescent multimodal imaging using <sup>68</sup>Ga-NOTA fluorescent silica nanoparticles could be used for sentinel node imaging using the PET/MRI scanner before surgery and for guiding surgeon to draining lymph nodes by the surgeon's view during the operation.

#### Molecular targeted imaging of cancer

We obtained 80~200 nm sized liposomes with encapsulated fluorescent substance (Cy5.5) and labeled with sugar chain (Sialyl Lewis X, SLX) in order to target to inflammation or tumor region, SLX-Lipo-Cy5.5 (GLYCOLIPO™-K1, Katayama Chemical Industry Co., Ltd, Japan). SLX is known to bind on E-selectin which is expressed on endothelial cells of vessel in the site of malignant tumor or active inflammation. We injected 200 µl of SLX-Lipo-Cy5.5 into CT26 tumor bearing mice via tail vein. The accumulation of SLX-Lipo-Cy5.5 was observed in the posterior, side, and ventral positions of mice using two different in vivo optical imaging systems, IVIS 100 (Caliper Life Science, Alameda, CA) and Maestro. Fluorescent signals were observed accumulation of the tumor region and liver in tumor bearing mice. These signals were observed significantly the highest at 48hr after tail vein injection in optical imaging system. As time goes by, fluorescent signals significantly decreased and also observed their efficient clearance from the body through renal clearance system. Radiolabeling of SLX-Lipo-Cy5.5 using I-131 labeled albumin for the therapeutic purpose is underway.

This biodegradable cancer targeted nano-liposome has a

## ABSTRACTS

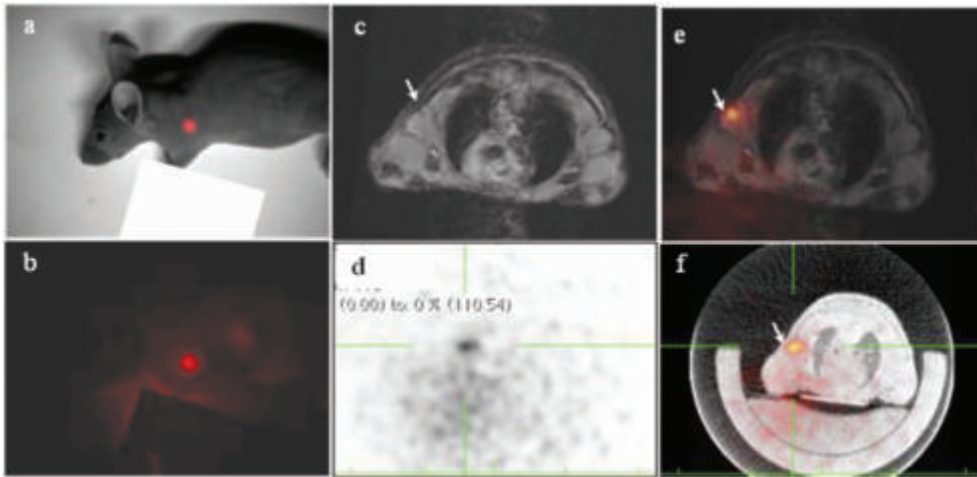


**Figure 1.** In vivo multimodal imaging of a mouse injected with Ga<sup>68</sup> labeled fluorescent nanoparticles. Axillary lymph node was detected by (a, b) Maestro, optical imaging system, (c) MRI and (d) PET (white arrow). PET signal was overlaid on (e) MRI and (f) CT image.

potential in molecular targeted diagnostic imaging and therapeutic applications.

If we combine nanotechnology and molecular imaging, we could guide surgeon for minimally invasive but accurately removal of tumor and personalized targeting therapy by validating the targeting efficiency using multimodal in vivo imaging.

096

**PBPK modeling for dosimetry of nonclinical and clinical radioimmunotherapy**

Prof. Kalevi Kairemo

Consultant in Nuclear Medicine, Clinical Chemistry & Pharmacology, Academic affiliation: Nuclear Medicine, Dept of Oncology, Helsinki University Central Hospital, Haartmaninkatu 4, FI-00029 HUS, Finland

Abstract not available

097

**Architecture & Music in the Light of Healing of Cancer Patients**

Dr. Gertraud Jestl-Horngache

University of Innsbruck, Innsbruck, Austria

Abstract not available

098

**Primary tumor size, can it predict the histopathologic outcome of an identified sentinel node?**

Gironella-Camomot Susan, Santiago Jonas, Magboo Vincent Peter

Nuclear Medicine Department, St. Luke 's Medical Center, Quezon city, Philippines

Background: Breast cancer is the most common malignancy in women. One of the treatment options is

axillary lymph node sampling by axillary lymph node dissection (ALND) to evaluate the lymph nodes which is associated with increased postsurgical morbidity. An alternative to ALND is sentinel lymph node (SLN) biopsy where most breast cancer patients are suitable for the procedure. Literatures show that the predictors of lymph node metastases include tumor size, tumor histopathology and patient age. Methodology: This is a retrospective study that will determine if there is a relationship between SLN positivity or negativity for malignancy spread and these predictors by reviewing the clinical profile of 20 female breast cancer patients who underwent radionuclide SLN mapping procedure, SLN and primary tumor biopsy in St. Luke's Medical Center from February 2004 to March 2008. Results: The mean age in years of the study group is  $51.8 \pm 13.6$ . Among the SLN, 15% is SLN (+) and 85% is SLN (-) for malignancy spread. Most of the SLNs are localized in the ipsilateral axillary region. The most common histologic type of primary tumor is invasive ductal carcinoma for both SLN (+/-). There is a direct relationship between SLN (+) and mean size of primary tumor and tumor aggressiveness. The SLN (+) has mean size of  $5.5 \pm 0.87$  cm, all of which have invasive ductal carcinoma as histologic diagnosis. Among the SLN (-) there exist an inverse relationship between tumor aggressiveness and size to predict a SLN (-) outcome. The SLN (-) has overall mean size of  $2.95 \pm 2.2$  cm, and is further grouped histologically into DCIS with mean size of  $3.87 \pm 3.33$  cm, invasive ductal carcinoma with  $2.5 \pm 0.38$  cm, and invasive papillary/micropapillary carcinoma with  $2.25 \pm 1.2$  cm. Conclusions: Invasive ductal carcinoma is the most common histologic type with the ipsilateral axillary region as the most frequent area of SLN localization. The combination of primary tumor size and histology may predict the SLN histologic outcome. Sentinel lymph node biopsy may obviate need for the invasive ALND in the accurate evaluation of patients who will undergo definitive surgical management.

099

**Evaluation of sentinel lymph nodes in patients with cutaneous malignant melanoma**

Lacic Miodrag, Lacic Mihovil, Stanec Mladen, Ivkic Mirko, Stanec Zdenko, Kusic Zvonko  
Dr. Lacic Private Practice, Zagreb, Croatia

**Aim:** The aim of this study was to evaluate the scintigraphic and sonographic characteristics of the sentinel lymph nodes (SLNs) in patients (pts) with cutaneous malignant melanoma (MM). **Methods:** Sentinel lymph node scintigraphy was performed in 181 pts, 82 female and 99 male, aged from 11 to 80 years (mean 50,01 years). Up to 74 MBq of Tc-99m nanocolloid were injected intradermally around the skin lesions (7 pts) or the biopsy scar (174 pts), followed by dynamic and static planar imaging until the SLNs became visible. The SLNs were marked on the skin using an external radioactive marker. Gray-scale sonography, followed by Color and Power Doppler analyses have been done using a 10 MHz linear probe. A hand held gamma probe was used for intra-operative mapping of SLN. **Results:** In 82, 45, 35 and 20 pts lesions were situated in the trunk, lower limbs, upper limbs and head and neck area respectively. SLNs were successfully detected in 180 from 181 pts on scintigraphy. 294 SLNs (1,65 per pts) were visualized on scintigraphy in 237 lymphatic basins (1,31 basins per pts). 148 regional lymphatic basins in 108 pts were evaluated sonographically. Sonography was unable to differentiate SLNs from surrounding tissue in 32% of pts. In 55% of pts SLNs had benign characteristics on sonography. SLNs changes suspected to be metastatic lesions were detected in 13% of pts on sonography. In 86% of these pts sonographically suspected metastatic lesions were histologically confirmed. 40% of pts with histologically proven SLNs metastasis had no sign of disease on sonography. A signal of increased blood flow within SLNs was detected in 7% of pts on Color and Power Doppler sonography. Among the operated pts 24% had positive SLN for MM. In 53% of these pts SLN was the only metastatic lymph node. **Conclusion:** Preoperative lymphoscintigraphic detection of SLNs followed by sonographic evaluation of drained lymphatic basins seems to be a reasonable diagnostic approach to the management of malignant melanoma.

100

**SPECT imaging in the diagnosis of pulmonary embolism, comparison with planar V/Q scan and CTPA**

Fatima Shazia Fatima, Fatima Arzoo Fatima, Irfan Javaid Irfan  
Nuclear Medicine, Nuclear Medicine Oncology and Radiology Institute, Islamabad, Pakistan

Although ventilation/perfusion (V/Q) lung scintigraphy is most frequently performed procedure for the diagnosis of pulmonary embolism, there is growing controversy about

its relevance, particularly due to the complexities in its reporting criteria and advancements in the multi slice CT scanning. Comparative studies between lung scanning and CTPA have already been performed, but their results were not impartial as the conventional planar perfusion scans were compared with tomographic images acquired using state-of-the-art CT scanners. The aim of our study was a balanced comparison between V/Q lung scintigraphy and CT angiography using advanced imaging techniques for both modalities. In addition we also compared the results of conventional planar lung V/Q scanning with SPECT results. **Methods:** A total of 45 patients with suspected pulmonary embolism were examined using V/Q lung scintigraphy in planar and SPECT technique as well as spiral CT. Ventilation scans were done using an 99mTc-DTPA aerosol. Two experienced referees assessed each of the 2 modalities. The final diagnosis was made at a consensus meeting while taking into account all of the imaging modalities, laboratory tests, clinical data, and evaluation of a follow-up period. **Results:** In the course of the consensus conference, pulmonary embolism was diagnosed in 25 of the 45 patients (56 %). Compared with planar scintigraphy, SPECT raised the number of detectable defects at the segmental level by 4 defects and at the subsegmental level by 23 defects. The sensitivity, specificity and accuracy of planar V/Q scintigraphy increased significantly after adding SPECT information. SPECT imaging showed superior sensitivity while CTPA had better specificity. **Conclusion:** SPECT imaging is a technical advancement that can substantially improve lung scintigraphy results. Lung SPECT scintigraphy and CTPA both yield an excellent and comparable diagnostic accuracy. Even though planar lung scintigraphy yields satisfactory results, it does not compare with tomographic imaging. SPECT lung scanning should be employed in all patients referred for suspicion of pulmonary embolism to give better results.

101

**Evaluation of performance of rest gated myocardial perfusion imaging in emergency room patients with suspected acute coronary syndrome presenting with acute chest Pain and non-diagnostic ECG - Preliminary results from the PREMIER trial**

Fatima Arzoo , Orellana Pilar, Better Nathan, Vitola Joao, Dondi Maurizio, Hyder S. Waqar  
Nuclear Medicine, INMOL, Lahore, Pakistan

Abstract not available

102

**Myocardial infarction, scar or ischemia at rest?**

Pirnazarov M, Rasulova N  
Nuclear Medicine, Republic Specialized Center of Surgery, Private Clinic "Samit", Tashkent, Uzbekistan

## ABSTRACTS

**Introduction:** It is common opinion that myocardial perfusion defects at rest are considered as areas of myocardial infarction or scar, however it is not always confirmed by ECG changes and clinical data. Aim: To exam the patients with myocardial perfusion defects according to myocardial perfusion scintigraphy at rest and with nitroglycerine to see if myocardial perfusion defects are true areas of myocardial infarction or scar. Material and methods: 40 patients (all males, mean age 49,75±12.46) with clinical manifestation of ischemic heart disease referred to balloon angioplasty and stents after angiography. Patients were divided into the two groups. 1st group - 18 patients with confirmed MI and 2nd group - 22 patients to whom MI could not be excluded rely upon on ECG and clinical data. To all patients myocardial perfusion scintigraphy (MPS) at rest and with had myocardial perfusion defects at rest according to myocardial perfusion scintigraphy (MPS). All of them nitroglycerine MPS on the next day after first examination was done. Results: According to our data out of 18 patients with confirmed MI in anamnesis on MPS with nitroglycerine 8 patients had non reversible perfusion defects on both at rest and with nitroglycerine. 10 patients had a partial reversible perfusion defects. Out of 22 patients with suspected MI according to clinical data, myocardial perfusion defects were found in all patients at rest, 11 patients had a full reversible myocardial perfusion defects and 9 had a partial reversibility and 2 patients had a worsening of myocardial perfusion with a “steal” syndrome in a better areas at rest. Conclusion: 27.5% patients with perfusion defects at rest had a reversible perfusion defects with nitroglycerine MPS that excludes them from the group of patients with MI and scars. Patients with full reversible defects according MPS with nitroglycerine have a benefit from revascularization.

103

#### **Carcinoma of Unknown Primary: Initial Experience with 18F FDG PET-CT**

Madhur Kumar Srivastava, Abhinav Jaimini, Madhavi Tripathi, Maria D'Souza, Rajnish Sharma, Anupam Mondal Deptt of Molecular Imaging and Research, INMAS, Delhi, India

**Aim:** In spite of increasing sophistication in the diagnostic workup for malignancies, detailed investigations fail to reveal a primary site of origin for a subset of patients with metastatic cancer. This is referred as Carcinoma of Unknown Primary syndrome (CUP). 18F FDG PET-CT, because of its sensitivity in detecting a large variety of carcinoma, appears to be suitable to detect unknown primary, the detection of which optimize patient's management and allow targeted therapy. Moreover the CT part of PET-CT by itself may also contribute by detection of PET negative findings. The incidence of CUP is between 2-9%. So we evaluated the role of 18F FDG PET-CT in

patients with CUP syndrome. Material and Methods: 57 patients with histologically proven metastatic disease were included in the study. 36 patient had cervical lymph node metastasis while rest had extracervical metastasis. All patients were evaluated with 18F FDG PET-CT, following the standard clinical and radiographic technique failing to establish any primary site and prior to endoscopy to localize any suspicious site. A whole body (Eye to thigh) 18F FDG PET-CT was performed 60 minutes after intravenous administration of 370 MBq of 18F FDG on the Discovery STE 16(GE) camera. Images were reconstructed into transaxial, coronal and sagittal views and viewed on a Xeleris workstation (GE). Images were evaluated visually and sites of abnormal /asymmetrical (for head and neck) FDG uptake were graded into three categories- Grade I: definitely abnormal pattern, Grade II: suspicious or equivocal, and Grade III: Negative/ no site localized. Furthermore all the patients were followed up for the period of 6-18 months. Results: The PET\_CT study suggested grade I uptake in 11 patients, grade II uptake in 15 patients and no uptake (grade III) in 31 patients. All grade I uptake were either endoscopically biopsied or underwent definitive Surgery and were histopathologically proved to be positive for carcinoma (Primary site). All grade II uptake were also biopsied but were negative for carcinoma on histopathology. In 30 patients, the PET-CT results were negative and no primary site was found on further investigations. All these patients were treated without localization of a primary site. One patient had FDG negative suspicious site in nasopharyngeal region on CT, which on histopathology proved to be nasopharyngeal carcinoma. 18F FDG PET-CT correctly identified the location of primary tumor in 11 patients (19.2%). Additional metastatic sites were found in 26 patients (45.6%). Conclusion: In this series of 57 patients with CUP, though 18F FDG PET-CT may not be very useful for initial diagnosis of the primary site but by identifying other sites of metastasis, it may be useful for post therapy follow-up and management of the cases

104

#### **Prediction of response to neoadjuvant chemotherapy in locally advanced breast cancer with scintimammography and its correlation with p-glycoprotein levels.**

Khan Muhammad Aleem, Munir Mudassara, Fatima Shazia, Irfan Javaid, Jameel Ghazal, Rafique Asif Nuclear Medicine, Nuclear Medicine Oncology and radiotherapy Institute, Islamabad, Pakistan.

**Background:** Neo-adjuvant chemotherapy (NACT) is one of the mainstays in the management regimen of locally advanced breast cancer (LABC) and showed promising reduction in mortality and morbidity statistics. Chemotherapeutic resistance is the result of complex interplay of genetic and molecular expressions. P-glycoprotein mediated mechanisms are the most studied

one and Tc-99m MIBI has been used in the functional evaluation of P-glycoprotein. Objectives 1. To measure tumour to background ratio (TBR), retention Index (RI), tumour kinetic rate (TKR) of Tc-99m-MIBI. 2. To compare the scintigraphic parameters with the mammographic measurements of tumor size before and after NACT, taken as gold standard. 3. To correlate the MDR-1 mRNA (multi-drug-resistance) measurements through PCR technique with scintigraphic measurements. Methods: 20 patients with LABC, candidates for NACT with no previous history of mastectomy or chemotherapy were included. All underwent mammograms of the diseased breast before and after NACT to measure the size of the lesion according to the RECIST (response evaluation criteria in solid tumours). All the patients then underwent scintimammography with 740 MBq Tc-99m-MIBI. Four sets of images were acquired at 15 minutes, 120 minutes, 180 minutes, and 240 minutes after the injection. Tumor to background ratios (T/B), retention index (RI) and tumour kinetic rates (TKR) were calculated. TKR was measured by exponential curve fitting to the decay corrected data of the tumour counts obtained at different time intervals. MDR-1 mRNA levels of all patients were measured with RT-PCR method. The patients then underwent three cycles of anthracycline based NACT. The patients with > 30 % reduction in tumor size on final mammographic image were labeled as responders (R) and rest as non responders (NR) to NACT. Results: The results showed 11 (55%) responders and 9 (45%) non responders. The RI measured at 2 & 3 hr did not show any significant difference ( $p > 0.05$ ). However, there was significant difference observed between the RI at 2 & 4 hrs and between 3 & 4 hrs ( $p < 0.05$ ). There was significant difference between the RI at 2 & 4 hrs, TKR between R & NR ( $p < 0.05$ ). The best predictive power of TBR was achieved at 4 hrs with a cut off of 2.5. For RI the best predictive powers were achieved at 2 hrs and for TKR it was achieved at mean +1 SD. There was a mean concordance of 53.3% between the scintimammographic parameters and MDR-1 mRNA expression. Conclusions: Response to neo-adjuvant chemotherapy for LABC can be predicted by scintimammography. Both the tumour kinetic rate and RI are the suitable parameters for predicting the response to NACT.

References:

1. Maini C. L., Technetium-99m-MIBI scintigraphy in the assessment of neoadjuvant chemotherapy in breast carcinoma *J. Nucl. Med.*, 38: 1546 1997.
2. Ciarniello A, et al. Tumor clearance of technetium-99m-sestamibi as a predictor of response to neoadjuvant chemotherapy for locally advanced breast cancer. *J Clin Oncol.* 1998; 16:1677

Kao CH, et al: P-glycoprotein and multidrug resistance-related protein expressions in relation to technetium-99m methoxyisobutylisonitrile scintimammography findings. *Cancer Res* 2001;61:1412, MDR-1 mRNA